MAGNESIA-SPINEL BRICK WITH GOOD COATING ADHESION AND HIGH RESISTANCE TO CORROSION AND SPALLING FOR CEMENT ROTARY KILNS

Makoto Ohno, Shogo Yoshikawa, Hitoshi Toda, Mikako Fujii, Hitoshi Chiba, and Fumihito Ozeki
MINO CERAMIC CO.,LTD., Nagoya, Japan

ABSTRACT

Recently, lining bricks in burning zone of cement rotary kilns have been severely damaged by clinker melt attack and thermal shock because they are exposed to unstable coating conditions due to increasing use of waste as fuels and raw materials.

Responding to varying operational conditions and increasing mechanical stress, we developed a magnesia-spinel brick that has good coating adhesion and high resistance to corrosion resistance and spalling. The developed brick demonstrated superior performance to our competitor's brick in actual kilns and has been highly valued by many customers.

INTRODUCTION

Zirconia-added magnesia-spinel bricks composed mainly of magnesia (MgO) and spinel ($MgO \cdot Al_2O_3$) are extensively used in burning zone of cement rotary kilns. This is because they can have both good coating adhesion and high corrosion resistance to the clinker melt while maintaining their high spalling resistance. Recently in Japan, however, the wear of the bricks has increased due to unstable coating conditions arising from the increasing use of alternative fuels and raw materials [1]. In order to improve the performance of the bricks in burning zone, we focused on the following three features, coating adherability, corrosion resistance, and spalling resistance, as characteristics required for harsh environments in burning zone.

In this paper we presented zirconia-added magnesia-spinel brick with high resistance to both corrosion and spalling as well as good coating adhesion. The developed brick exhibited excellent properties in laboratory tests and field trials, which is attributed to high content of MgO, enhanced bonding in the matrix and dense microstructure as well as effect of ziconia.

INFLUENCE OF ALTERNATEIVE FUELS AND RAW MATERIALS ON THE REFRACTORIES

Generally the cement coating protects the lining bricks from being exposed to high temperatures and liquid phase of cement raw meals in burning zone. Figure 1 shows the appearance of the inside of past (25 years ago) and present cement kilns immediately after the shutdown. As seen in Figure 1, the coating is thinner nowadays. Although the state of coating adhesion is observed at the time of shutdown, the coating is likely to be thinner when the kiln is operating. The reason for this is that as a result of increasing use of alternative fuels and raw materials SO_3 content even in burning zone increases and SO_3 combines with CaO to form $CaSO_4$, leading to the reduction of liquid viscosity [2] and increasing amount of liquid phase. Excess of low viscosity liquid phase appears to inhibit the formation of thick coating. To identify the recent environmental change in burning zone, we calculated the molar ratio of sulfur/alkali of used bricks by using the following formula.

Fig. 1: Appearance of inside of past (25 years ago) and present cement kilns immediately after shutdown.

$$\text{Molar ratio of sulfur/alkali} = \frac{SO_3/80}{(K_2O/94+Na_2O/62)-Cl_2/71}$$

This formula is based on the following series of reaction according to thermodynamic principle. Alkalis such as K_2O combine first with chlorine to form alkali salts and then if excess alkalis are remaining, alkalis combine with sulfur to form alkali sulfates such as K_2SO_4. Sulfur in excess of alkali combines with CaO to form $CaSO_4$. This formula is often applied to upper transition bricks but we utilize it to evaluate burning zone conditions.

Figure 2 shows the shift in molar ratio of sulfur/alkali of used bricks in burning zone, which were sampled at several shutdowns in two plants for the past five years (L/D=2.3 in Plant A and L/D=1.3 in Plant B). L/D represents the position from the kiln outlet divided by the kiln diameter. Chemical compositions of the total infiltrated minerals for each sample brick were measured and normalized by its remaining thickness and service period. All the samples were used for half a year, approximately 4,000 hours. The graph clearly shows that as for Plant A molar ratio of sulfur/alkali increases at the time between 2013 and 2015. As for Plant B, molar ratio of sulfur/alkali also tends to increase at the time after 2016. In order to confirm the influence of SO_3 content increase on the lining bricks at the burning zone, we studied the wear rate in Plant A.

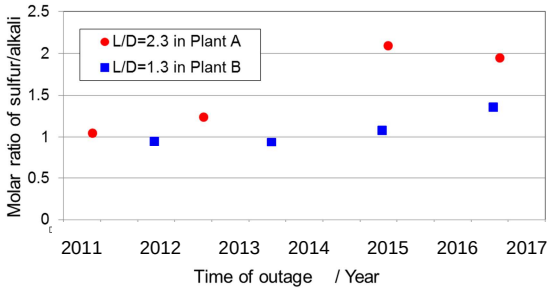

Fig. 2: Shift in molar ratio of sulfur/alkali of used bricks in burning zone (L/D=2.3 in Plant A and L/D=1.3 in Plant B)

Figure 3 shows the shift in wear rate of lining bricks at L/D of 1.3 to 3.3 in Plant A kiln. We see from Figure 3 that at the area from 2 to 3.5 the wear rate for Apr. 2015 and Nov. 2016 increased compared to Apr. 2011 and Nov. 2012. That is the timing when the molar ratio of sulfur/alkali of the sample went up. According to the Plant A staff, they increased the utilization of petcoke on the kiln burner at that time. Therefore, the increase of SO_3 content in burning zone may have caused unstable coating conditions, leading to the wear rate increase.

We have recently seen some cases of wear rate increase in burning zone as shown above, so we worked on the development of highly resistant burning zone brick.

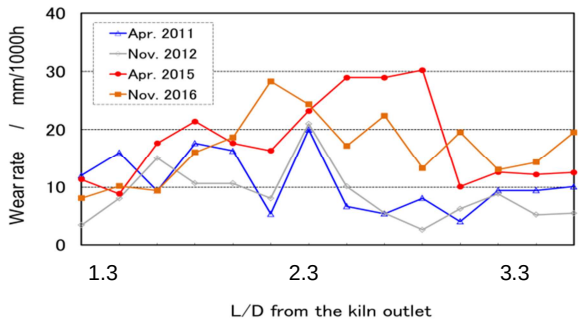

Fig. 3: Shift in wear rate of lining bricks at L/D of 1.3 to 3.3 in Plant A kiln

CONCEPTS OF BURNING ZONE BRICK

1. Good coating adhesion

-Enhancing the coating adherability by adding a combination of special raw materials to a magnesia-spinel based brick containing dead burned magnesia and small spinel grains

2. High corrosion resistance

-Boosting the corrosion resistance by increasing MgO content and developing the matrix bonding with addition of special raw materials

3. High spalling resistance

-Boosting the spalling resistance by blending spinel materials with proper sizes and in proper proportions

DEVELOPMENT OF BURNING ZONE BRICK

1. Good coating adhesion

In order to evaluate the coating adherability of the basic bricks, we performed the following test.

30g of coating agent (cement raw meal: 90%, K_2SO_4: 5%, pulverized coal: 5%) was pressed into a cylinder 30mm in diameter. The agent was placed on the surface of a specimen with 60×60×30mm dimension. The specimens were heated up to 1450°C and maintained for 3 hours. After the cooling, the adherability was evaluated by taking off the agent with a hand as illustrated in Figure 4 and then cutting the specimens and observing the cross section close to the boundary surface.

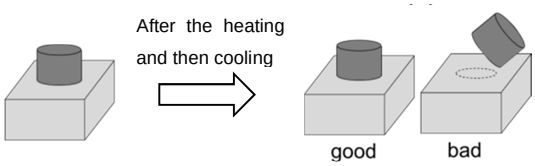

Fig.4: Illustration of the coating adhesion test

Table 1 shows a summary of the test results together with the properties of the specimens. Figure 5 and 6 show the cross section and its microstructure of specimen A and C after the test. Infiltration depth indexes were determined based upon the infiltration depth of specimen A which was converted to 100. The infiltration depth was measured by SEM. The results indicate zirconia addition improved the adherability and reduced the infiltration of the agent constituents. Furthermore, zirconia addition tends to increase the cold crushing strength, which is most likely caused by matrix bonding development. Specimen C demonstrated the best coating adherability and the least infiltration of all.

Tab. 1: Test results of the coating adhesion test and the properties of the specimens

Specimens	A	B	C
Additive X	○		○
Zirconia addition		○	○
Apparent porosity / %	15.2	15.8	14.8
Bulk density / g·cm^{-3}	3.00	2.98	3.01
Cold crushing strength / MPa	42	43	45
Coating adhesion test	bad	average	good
Infiltration depth index	100	51	49

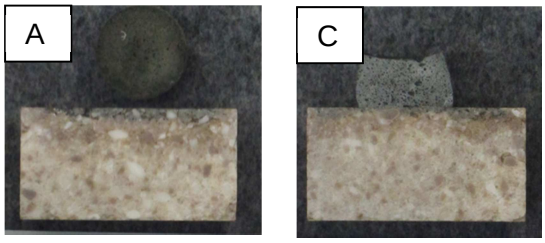

Fig. 5: Cross section of specimen A and C after the coating adhesion test

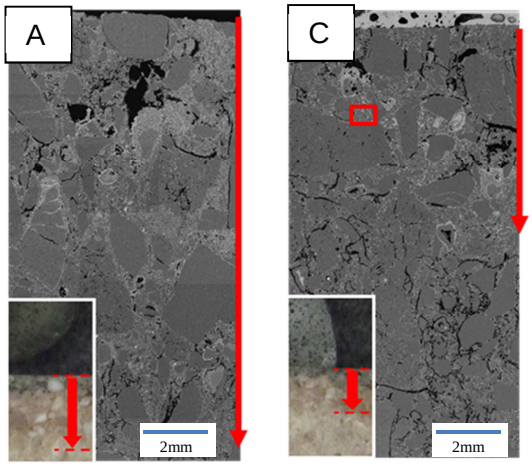

Fig. 6: Microstructure of specimen A and C near the boundary surface after the coating adhesion test

Figure 7 shows the EDS elemental mapping of specimen C in the vicinity of the boundary surface, which is represented with a red square in Figure 6. From the detailed EDS analysis, in specimen A $CaO\text{-}SiO_2$ and $CaO\text{-}Al_2O_3$ minerals were found to infiltrate up to 11mm depth with the structure deterioration. On the other hand, it was observed in specimen C that $CaO\text{-}Al_2O_3\text{-}SiO_2$ minerals infiltrated in the matrix and its depth

was reduced up to 5.5mm. In the reaction of magnesia-spinel brick with main cement constituent (CaO), liquid phase is relatively hard to generate in some composition but generates rapidly in other composition [3], which indicates excessive amounts of liquid phase may generate, infiltrate, and corrode the brick under certain condition. The possible reason for less infiltration in specimen C is that calcium zirconate reacted with cement constituents and retarded the rapid formation of low viscosity liquid phase mainly composed of calcium aluminate. Also, additive X may have facilitated the generation of viscous liquid phase but inhibited the infiltration, resulting in the best coating adherability. Furthermore, the dense microstructure with matrix bonding development probably contributed to reduction of deep infiltration.

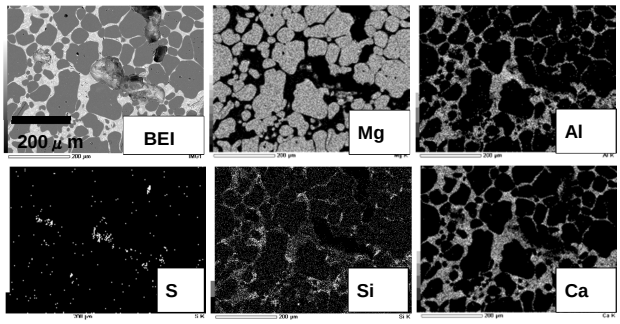

Fig. 7: EDS elemental mapping of specimen C in the vicinity of the boundary surface, which is represented with a red square in Fig. 6

2. High corrosion resistance

A rotary drum corrosion test was conducted to evaluate the corrosion resistance of the specimens. The schematic view of rotary drum corrosion test apparatus is illustrated in Figure 8.

The specimens were heated up to 1800°C for 5 hours and maintained for 1 hour with 1kg of test slug (cement raw meal: 85%, K_2SO_4: 5%, pulverized coal: 5%, alumina cement: 5%). After that, the burner was turned down. The temperature was decreased to approximately 1000°C. The specimens were heated again up to 1800°C. This manipulation was repeated 8 times over three days.

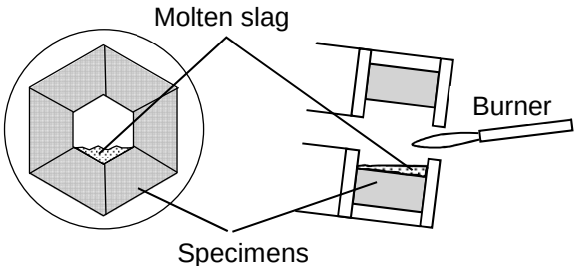

Fig. 8: Schematic view of rotary drum corrosion test

Cross sections of specimen A and C after the test are shown in Figure 9. Specimen C demonstrated less corrosion than A. Additionally, specimen C showed no spalling whereas some portion was spalled in A. We speculate that synergy effect of high content of magnesia (approx. 90%) and the dense microstructure enhanced the corrosion resistance of specimen C.

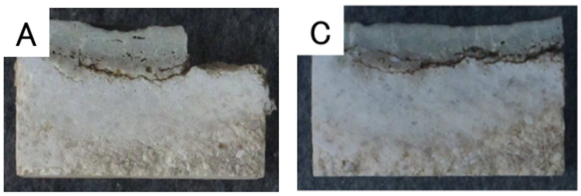

Fig. 9: Cross sections of specimen A and C after the rotary slag test

3. High spalling resistance

All specimens (A,B and C) have high flexibility as they are created based on our spinel technology. Thus all of them exhibit low modulus of elasticity and high thermal shock resistance. Here we show the thermal shock resistance of specimen C in comparison with a magnesia brick made by conventional technology.

A specimen with 80×80×230mm dimension was inserted into a furnace maintained at 1300℃ and heated while making one-third of the specimen in rectangular direction outside the furnace. The specimen was kept for 15 minutes and then taken out. The heated side was soaked for three minutes in a water bath with 60mm depth and then taken out. After that, the specimen was kept in air for 12 minutes. This manipulation was repeated 3 times.

Figure 10 shows the cross section of specimen C after the test in comparison with a Magnesia-Spinel brick containing 90% MgO made by conventional technology. Specimen C showed no definite crack whereas the conventional brick showed many cracks in the position from the top to 70mm. Microcracks and the distributed fine spinels, our spinel technology, presumably contributed to high thermal shock resistance.

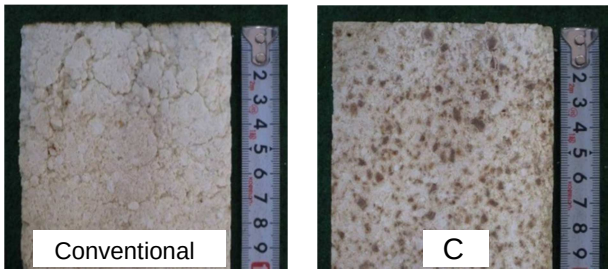

Fig. 10: Cross sections of specimen C and magnesia-spinel brick made by conventional technology after the thermal shock resistance test

APPLICATION OF THE DEVELOPED MAGNESIA -SPINEL BRICK TO ACTUAL KILN

We developed a zirconia-added magnesia-spinel brick, based on specimen C, and applied it to burning zone in actual kilns. Typical properties of the developed brick are shown in Table 2.

Tab. 2: Typical properties of developed brick based on specimen C

Apparent porosity /%	14.8
Bulk density /g·cm^{-3}	3.01
Cold crushing strength /MPa	48
Modulus of elasticity /GPa	31
Chemical composition /mass%	
MgO	89

Figure 11 shows the cross section of the developed brick used at 2.8 of L/D in a calciner kiln with 5.8m ID for approximately 4,000 hours in comparison with a competitor's brick (hereinafter referred to as other's brick) used at 3.0 of L/D for the same period. The wear of the developed brick was only 30mm and no crack and damage was observed throughout the brick. The remaining thickness of the developed brick was 30 to 40 mm bigger than that of the other's brick. Furthermore, the developed one demonstrated no corroded surface whereas the other's one showed flat surface with slight corrosion by clinker melt.

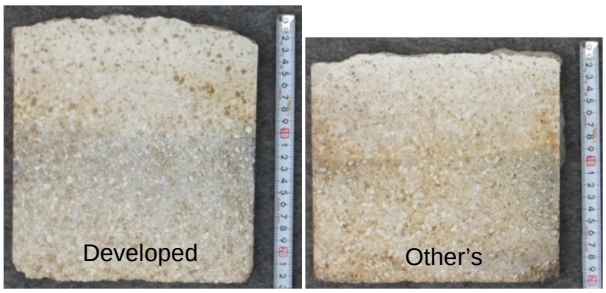

Fig. 11: Cross sections of the developed brick (left) and the other's brick (right) used at 2.8 and 3.0 of L/D respectively, which was used for approximately 4,000 hours in the burning zone in a calciner kiln

Table 3 shows the measured results of physical properties and XRD of both bricks according to layer divisions of 30mm each from the hot face. Figure 12 shows the measured results of chemical composition (infiltrated constituents) of each layer of both bricks. Few infiltrated and reacted minerals were observed in the developed brick while some minerals such as KCl, $K_2Ca_2(SO_4)_3$ were observed in the other's brick. Furthermore, $2CaO \cdot MgO \cdot 2SiO_2$, which is a mineral generated by the reaction of brick with cement, was confirmed at the first layer. These results indicate that the developed brick demonstrated high corrosion, infiltration, spalling resistance as well as excellent coating adherability, leading to prevention of wear.

Tab. 3: Measurement results of the developed brick and the other's brick used at L/D of 2.8 and 3.0 respectively

Developed brick

Layer	1	2	3	4	5	6,7
Distance from hot face / mm	0-30	30-60	60-90	90-120	120-150	150-220
Physical properties						
Apparent porosity/ %	12.5	13.9	14.3	14.3	13.9	13.9
Bulk density/g・cm^3	3.06	3.04	3.04	3.04	3.05	3.05
Infiltrated minerals						
KCl	(-)					

Other's brick

Layer	1	2	3	4	5	6
Distance from hot face / mm	0-30	30-60	60-90	90-120	120-150	150-188
Physical properties						
Apparent porosity /%	10.8	9.8	13.9	16.7	16.7	16.5
Bulk density /g・cm^3	3.03	3.08	2.99	2.95	2.94	2.95
Infiltrated minerals						
KCl	-	-	(-)			
$K_2Ca_2(SO_4)_3$	(-)					
$2CaO \cdot MgO \cdot 2SiO_2$	(-)					

Note: X-ray Intensity: Strong XXXXX > XXXX > …> X > x > - > (-) Weak

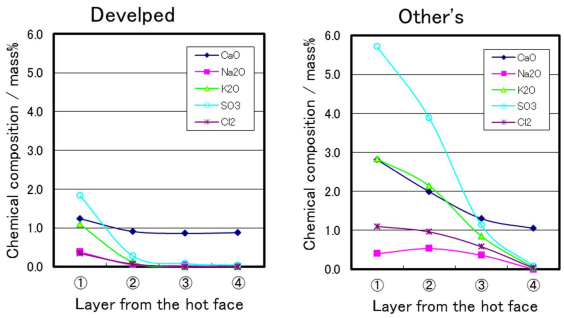

Fig. 12: Measurement results of chemical composition (infiltrated constituents) of the developed brick and the other's brick

CONCLUSION

As a result of increasing use of alternative fuels and raw materials increase of SO_3 content in lining bricks even in burning zone has been observed. This environmental change is most likely to cause unstable coating conditions in burning zone. Responding to recent harsh conditions, we developed a zirconia-added magnesia-spinel brick that has good coating adhesion, high corrosion and spalling resistance, which is attributed to high content of MgO, enhanced bonding in the matrix and dense microstructure as well as effect of ziconia. The developed brick exhibited excellent properties in actual kilns and highly valued by many customers. The use of it has been expanding throughout Japan. We will continue to improve the refractories and supply quality products to loyal customers.

REFERENCES

[1] Makoto Ohno, Shogo Yoshikawa, Yoshiharu Kajita, and Yoshio Mizuno : Taikabutsu, 66[9] 464-470 (2014)
[2] V.M. Moorthy : World Cement, Dec. 73-75(2003).
[3] Toru Honda : Doctoral thesis, Shizuoka university, 58-64 (2003)